Three-dimensional optical trajectory tracing and energy deposition of a laser beam in a laser-driven fusion

Shi-Bing Liu,[1,2] Ping-Qing Luo,[2] Yong-Hui Zhang,[2] Shao-Ping Zhu,[2] and Wei-Yan Zhang[2]
[1]*CCAST (World Laboratory), P. O. Box 8730, Beijing 100080, China*
[2]*Institute of Applied Physics and Computational Mathematics, P. O. Box 8009, Beijing 100088, China**
(Received 7 September 2000; revised manuscript received 29 November 2000; published 27 February 2001)

A convenient method of three-dimensional ray tracing is suggested in the geometrical optical approximation, in which the laser ray propagation is completely based on the concept of optical trajectory tracing rather than depending upon the effective force and propagation time. This tracing has two obvious advantages that the direct application of Snell's law can be avoided when a ray crosses a different density zone and that to any desired accuracy it takes much less computation time than existing tracing. For Gaussian light beam propagation, in a spherically symmetric plasma atmosphere, the results emphasize that the deposition uniformity is strongly dependent not only on the wavelength of the laser but also on the temperature of the plasma.

DOI: 10.1103/PhysRevE.63.036703 PACS number(s): 07.05.Tp, 02.60.Lj

I. INTRODUCTION

In laser-driven initial confinement fusion [1], the deposition of laser energy and the uniformity of energy absorption by plasma are critical stages in achieving a high gain and symmetric implosion of a spherical pellet [2,3]. Unfortunately, to calculate the energy deposition by solving the full wave equation of the laser light is extremely difficult for a multidimensional density profile of the plasma. The energy deposition is computed in practice by tracing laser rays through the plasma by the geometrical optical approximation and energy absorption along the ray trajectory by inverse bremsstrahlung (IB) and resonance excitation or other absorption mechanisms. The validity of tracing by the geometrical optics approximation is based on the facts that the light wavelength is much shorter than the plasma scale length and the electron density varies slowly over the laser wavelength.

In geometrical optical theory, the local electromagnetic wave phase $\psi(\mathbf{r})$ in nonhomogeneous media is assumed to be a complex function. The eikonal equation is $(\nabla\psi)^2=\eta^2$, where $\eta=\eta(x,y,z)$ is the local refractive index in the medium. The ray equation in the geometrical optics approximation is represented as [4–6]

$$\frac{d^2\mathbf{r}}{dt^2}=\frac{1}{2}\nabla(\eta^2c^2), \tag{1}$$

where $\mathbf{r}$ is the position vector, t the propagation time, and c the speed of light. In a nonrelativistic unmagnetized plasma for an incident light wave with frequency ω, $\eta=(1-\omega_p^2/\omega^2)^{1/2}=(1-n_e/n_c)^{1/2}$ and is assumed to vary on a much longer spatial scale than the light wavelength. Where ω_p, n_e, and n_c are the characteristic frequency, the density, and the critical density of plasma electrons, respectively. In such a framework the wave fronts with wave vector $\mathbf{k}$ move at the phase velocity $\omega|\mathbf{k}|^{-1}=c|\nabla\psi|^{-1}$. The ray is considered to be under the influence of an effective force $\sim -\frac{1}{2}(\nabla\delta n)c^2$, where $\delta n=n_e/n_c$ and to move at the group velocity $\mathbf{v}_g=\partial\omega/\partial\mathbf{k}=c\nabla\psi$; it carries the corresponding laser energy. Based on this concept recent work [6] gave a method of tracing using an unstructured three-dimensional (3D) grid. It is an extremely complicated determination of where rays cross computational zone interfaces. This originates from the discontinuous density at zone interfaces which cause singularities in the effective force governing ray propagation. The application of Snell's law at the zone interfaces is the only way to treat these singularities. However, for a multidimensional discontinuous plasma-density profile (given by hydrodynamic codes) it is very inconvenient.

In this paper we propose a more direct 3D ray equation and a more convenient ray-tracing method in the approximation of geometrical optics. By using optical trajectory tracing the conceptions of ray velocity, effective force, and tracing time are avoided. In particular, the clear advantage of this tracing method is that the direct application of Snell's law can be left out and it requires much less computational effort (in comparison with existing methods) for obtaining any desired accuracy. For an incident Gaussian light wave we calculate the laser energy deposition and examine the uniformity of absorption. The results stress that the absorption efficiency and the deposition uniformity are strongly dependent on the plasma temperature as well as the light wavelength.

II. RAY EQUATION AND TRACING

According to Fermat's principle [7,8], another form of the ray equation in a graded-index medium, in the geometrical optical approximation, is

$$\frac{d}{ds}\left[\eta(\mathbf{r})\frac{d\mathbf{r}}{ds}\right]=\nabla\eta(\mathbf{r}), \tag{2}$$

where ds is an element of the arclength along the ray. For the convenience of direct numerical integration of the above equation, a new variable ξ is defined as $d\xi=ds/\eta$. Equation (2) thus becomes

*Mailing address.

$$\frac{d^2\mathbf{r}}{d\xi^2}=\frac{1}{2}\nabla(\eta^2). \tag{3}$$

Further, defining an optical ray vector as $\mathbf{R}\equiv d\mathbf{r}/d\xi$, the ray equation is simplified to a first-order differential equation,

$$\frac{d\mathbf{R}}{d\xi}=\frac{1}{2}\nabla(\eta^2). \tag{4}$$

It is obvious that the components of this vector are the three optical direction cosines, namely,

$$\mathbf{R}=\eta\frac{d\mathbf{r}}{ds}=\mathbf{e}_x\eta\cos\alpha+\mathbf{e}_y\eta\cos\beta+\mathbf{e}_z\eta\cos\gamma,$$

where α, β, and γ are the angles that the ray direction makes with the x, y, and z axes, respectively. One can see from the ray equation (4) that the optical ray vector $\mathbf{R}$ is obtained simultaneously with the propagation process, which simplifies the computation of refraction at various optical surfaces. The convenience is obvious for ray tracing especially in a multidimensional random plasma-density profile. In this situation Snell's law can be written in terms of the optical ray vector simply as $\mathbf{R}_a=\mathbf{R}_b+\sigma\mathbf{e}_N$, where $\mathbf{R}_b$ and $\mathbf{R}_a$ are the optical ray vectors before and after refraction, respectively, and $\mathbf{e}_N$ is the unit vector normal to the optical surface at the point of refraction. The parameter $\sigma=(\eta_a^2-\eta_b^2+\kappa)^{1/2}-\kappa$, where η_b and η_a are the refractive indices of the two media involved in refraction at the point of refraction, and κ is the scalar product of $\mathbf{R}_b$ and $\mathbf{e}_N$. The other convenience is that the propagation time of the ray is not involved in Eq. (4) unlike the ray equation (1). Direct optical trajectory tracing (not time tracing) and simplification of the computation of refraction can reduce the computational time for the tracing process. If we write the vector $\mathbf{R}$ as the component forms

$$R_x=\frac{dx}{d\xi},\quad R_y=\frac{dy}{d\xi},\quad R_z=\frac{dz}{d\xi}, \tag{5a}$$

then the ray equation (4) becomes

$$\frac{dR_x}{d\xi}=\frac{1}{2}\frac{\partial\eta^2}{\partial x},\quad \frac{dR_y}{d\xi}=\frac{1}{2}\frac{\partial\eta^2}{\partial y},\quad \frac{dR_z}{d\xi}=\frac{1}{2}\frac{\partial\eta^2}{\partial z}, \tag{5b}$$

which can be directly integrated numerically by the standard Runge-Kutta method [9]. Information about the laser-plasma interaction, e.g., the properties of collision and response of the plasma, etc., can be included in the function $\eta^2(\mathbf{r})$ due to the relation $\epsilon=\eta^2$, where ϵ is the dielectric function.

These characteristics of ray equation (4) make ray tracing extremely easy. Which zone the ray will enter can be determined by simple logical judgment alone, and then the ray will arrive at the next point *automatically* in terms of Snell's law when a ray passes from one computational zone to another.

In order to carry out ray tracing, we assume that the scale length of the electron-density gradient is of the same order as the grid size, the gradient is constant while a typical ray traverses the grid, and the mesh face is planar. However, the density and gradient are usually not followed with an evolution equation because the hydrodynamic codes discretize the fundamentional equations on meshes of points that define computational nodes and zones, i.e., some computed quantities are specified in the zones and others are specified at nodes. The mesh number is usually represented by a specified node number $i=1,2,3,\ldots$. In the ith computational zone the electron density $n_e^i(x,y,z)$ is determined by the specified values at each contiguous node. According to planar geometrics, therefore, the zone density can be roughly represented as

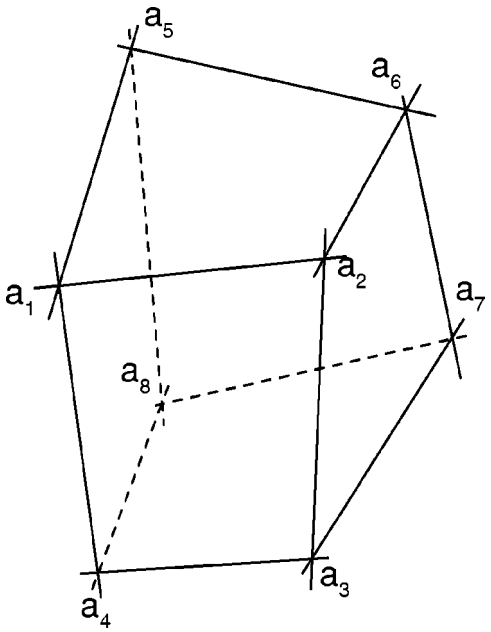

FIG. 1. Geometry of one 3D computational mesh.

$$n_e^i=\hat{n}_e^i+\frac{\partial n_e^i}{\partial x}(x-x_i)+\frac{\partial n_e^i}{\partial y}(y-y_i)+\frac{\partial n_e^i}{\partial z}(z-z_i) \tag{6}$$

and the relevant gradients are

$$\frac{\partial n_e^i}{\partial x}=-\frac{1}{3}\sum_{P_j,j=1}^{3}\frac{\Delta_{yz}(P_j)}{\Delta(P_j)}, \tag{7a}$$

$$\frac{\partial n_e^i}{\partial y}=-\frac{1}{3}\sum_{P_j,j=1}^{3}\frac{\Delta_{zx}(P_j)}{\Delta(P_j)}, \tag{7b}$$

$$\frac{\partial n_e^i}{\partial z}=\frac{1}{3}\sum_{P_j,j=1}^{3}\frac{\Delta_{xy}(P_j)}{\Delta(P_j)}, \tag{7c}$$

where $P_j(j=1,2,3)$ represent three faces connected to the i node, $\hat{n}_e^i(x_i,y_i,z_i)$ is the i-node density, and x_i, y_i, and z_i are the coordinates of this node. As an example of node geometry we give a computational zone $(i=1)$ in Fig. 1. The zone density $n_e^1(x,y,z)$ is represented by the density $\hat{n}_e^1(x_1,y_1,z_1)$ at node a_1. The three faces connected to node a_1 are $P_1(a_1,a_2,a_3,a_4)$, $P_2(a_1,a_2,a_6,a_5)$, and

$P_3(a_1,a_4,a_8,a_5)$. For the P_1 face where the node densities are written as $\hat{n}_e^1$, $\hat{n}_e^{a_2}$, $\hat{n}_e^{a_3}$, and $\hat{n}_e^{a_4}$ at nodes $a_1=a_1(x_1,y_1,z_1)$, $a_2=a_2(x_{a_2},y_{a_2},z_{a_2})$, $a_3=a_3(x_{a_3},y_{a_3},z_{a_3})$, and $a_4=a_4(x_{a_4},y_{a_4},z_{a_4})$, respectively, the corresponding coefficient determinants can be represented as

$$\Delta(P_1)=\begin{vmatrix} x_{a_2}-x_1 & y_{a_2}-y_1 & z_{a_2}-z_1 \\ x_{a_3}-x_1 & y_{a_3}-y_1 & z_{a_3}-z_1 \\ x_{a_4}-x_1 & y_{a_4}-y_1 & z_{a_4}-z_1 \end{vmatrix}, \tag{8a}$$

$$\Delta_{xy}(P_1)=\begin{vmatrix} x_{a_2}-x_1 & y_{a_2}-y_1 & \hat{n}_e^{a_2}-\hat{n}_e^1 \\ x_{a_3}-x_1 & y_{a_3}-y_1 & \hat{n}_e^{a_3}-\hat{n}_e^1 \\ x_{a_4}-x_1 & y_{a_4}-y_1 & \hat{n}_e^{a_4}-\hat{n}_e^1 \end{vmatrix}, \tag{8b}$$

$$\Delta_{yz}(P_1)=\begin{vmatrix} y_{a_2}-y_1 & z_{a_2}-z_1 & \hat{n}_e^{a_2}-\hat{n}_e^1 \\ y_{a_3}-y_1 & z_{a_3}-z_1 & \hat{n}_e^{a_3}-\hat{n}_e^1 \\ y_{a_4}-y_1 & z_{a_4}-z_1 & \hat{n}_e^{a_4}-\hat{n}_e^1 \end{vmatrix}, \tag{8c}$$

$$\Delta_{zx}(P_1)=\begin{vmatrix} z_{a_2}-z_1 & x_{a_2}-x_1 & \hat{n}_e^{a_2}-\hat{n}_e^1 \\ z_{a_3}-z_1 & x_{a_3}-x_1 & \hat{n}_e^{a_3}-\hat{n}_e^1 \\ z_{a_4}-z_1 & x_{a_4}-x_1 & \hat{n}_e^{a_4}-\hat{n}_e^1 \end{vmatrix}. \tag{8d}$$

The temperature and relevant gradient of the electron, in the same way as above, can also be obtained. These results agree with those of Ref. [6].

III. CALCULATION OF ENERGY DEPOSITION

To compute the energy deposition it is necessary to consider the spatial distribution of laser intensity. Assuming an incident Gaussian beam propagating along the z axis, as a zero-order mode, the beam intensity is written as

$$I_r(x,y,z)=\frac{I_0}{w(z)}\exp\left[-2\frac{x^2+y^2}{d_f^2 w(z)}\right], \tag{9}$$

where I_0 is the focused intensity, d_f the radius of the focal spot, and $w(z)=1+(z\lambda/\pi d_f^2)^2$ is dependent on the laser wavelength λ.

Assuming that the maximum intensity of incident rays at the point of passing from vacuum to the plasma atmosphere is $I_{\rm im}$, the intensity absorbed by electrons as the ray finishes one step along the path ($s_i-s_{i-1}=\Delta s_i$), due to the IB process, can be written as

$$\Delta I_{\rm IB}^i=I_{i-1}-I_i=I_{\rm im}(1-\chi_i)\chi_1\chi_2\cdots\chi_{i-1}, \tag{10}$$

where I_i is the residual intensity of the ray at the ith step and χ is the IB absorption rate, namely,

$$\chi_i=\exp\left(-\int_{\Delta s_i}K_i ds_i\right). \tag{11}$$

The IB absorption coefficient K is dependent on the electron density and temperature at the computational point, and is expressed as [10]

$$K\simeq 10^{21}K_0\frac{\delta n^2}{\lambda^2}(1-\delta n)^{-1/2}, \tag{12}$$

where

$$K_0=\left[\left(\frac{4}{3}\right)\left(\frac{2}{\pi m_e}\right)^{1/2}\frac{e^4 Z}{c}\right]T_e^{-3/2}\ln\Lambda, \tag{13}$$

and Z is the ion charge number, e the electron charge, m_e the electron mass, $\ln\Lambda$ the Coulomb logarithm, and the temperature T_e is in eV. The term in Eq. (12), $(1-\delta n)^{-1/2}$, in fact, is important only for $\omega\simeq\omega_p$ (resonance excitation) and hence one can neglect it in calculation of IB absorption because this term only increases K. Once the absorption rate is obtained it can be integrated along the ray trajectory to determine the fraction of energy deposited in the computational zone.

As an application of the above theory, we compute the energy deposition in a spherical target associated with direct drive laser fusion. In practice, the calculation is greatly simplified by using beams with identical, azimuthally symmetric intensity profiles. Then only one beam must be calculated and results for the other beams are obtained by rotation. We assume that the incident laser beam is focused on the center of the spherical fusion pellet, the wavelength $\lambda=1.06$ μm, the radius of the spherical plasma is $R=10$ mm, and the critical density point along the z axis is $z_c=3$ mm. In the computations one beam is split into 200 rays along the y direction and only 100 rays are taken into account due to azimuthal symmetry. Defining the deposited fraction as $\Delta I/I_0$, the fraction of IB absorption for the first 20 rays from the beam axis vs the propagation depth z is plotted in Fig. 2 at 100 eV and 2 keV electron temperatures. The result shows that the energy deposits rapidly in the corona and is completely depleted in a short path [Fig. 2(a)]. When the temperature increases continuously the deposition length increases, and if it approaches or exceeds the keV level the deposition efficiency becomes so low that part of the energy is reflected back into the vacuum [Fig. 2(b)]. It is obvious that the deposition is strongly dependent on the temperature, implying that a low electron temperature is of great advantage for the rate, efficiency, and uniformity of the energy deposition.

Resonance absorption is possible only for the p-polarization component of the laser field when the beam propagates from the turning to the critical points. However, for electron temperatures below the keV level, from the above result, resonance absorption does not exist because the energy is completely depleted before the rays arrive at the turning point. If the electron temperature approaches or exceeds the keV level the resonance absorption could occur as the incident rays depart from the beam axis. For convenience, the electron density from the turning point r_t (where the density is n_t) to the critical surface r_c is assumed to have a linear profile [11]. Then the resonance absorption rate is

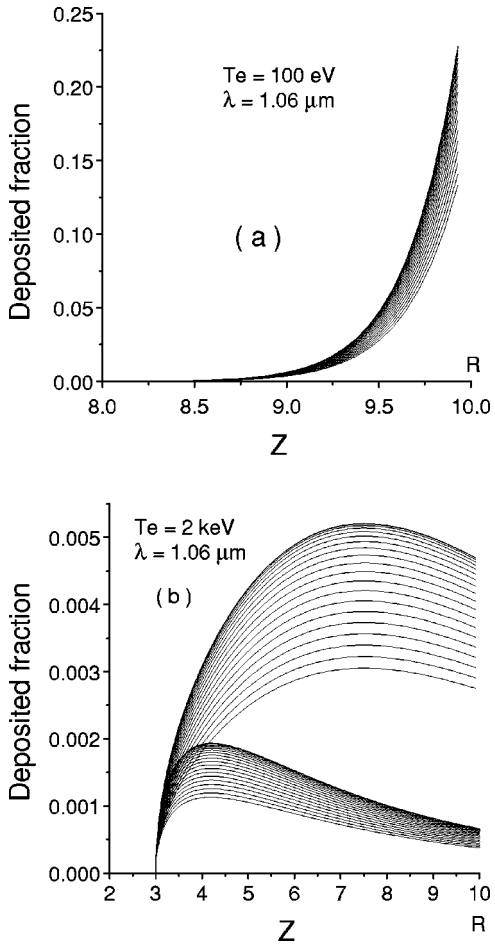

FIG. 2. Deposited fraction of IB absorption vs propagating depth of ray with wavelength 1.06 μm for (a) 100 eV and (b) 2 keV electron temperatures.

$$\chi_r = \frac{\phi^2(\tau)}{2}, \quad \tau = \left(\frac{2\pi L}{\lambda}\right)^{1/3} \sin\theta_0, \tag{14}$$

and the density scale length is

$$L = \frac{r_t - r_c}{1 - \delta n_t}. \tag{15}$$

In these equations the incident angle θ_0 is governed by ray tracing, $\delta n_t = n_t / n_c$, and the resonance function is described as

$$\phi(\tau) \simeq 2.3\tau \exp\left(-\frac{2\tau^3}{3}\right). \tag{16}$$

Figure 3 plots the fraction of resonance absorption at different azimuthal angles. The maximum fraction absorbed due to resonance exceeds that of IB absorption by 40% for azimuthal angle $\phi = \pi/2$ and zero for $\phi = 0$, which shows an obvious deposition nonuniformity. This implies that the resonance absorption is the main dynamical reason leading to nonuniformity of the energy deposition.

The wavelength dependence of energy deposition is shown in Fig. 4. By comparison with Fig. 2(b) one can see

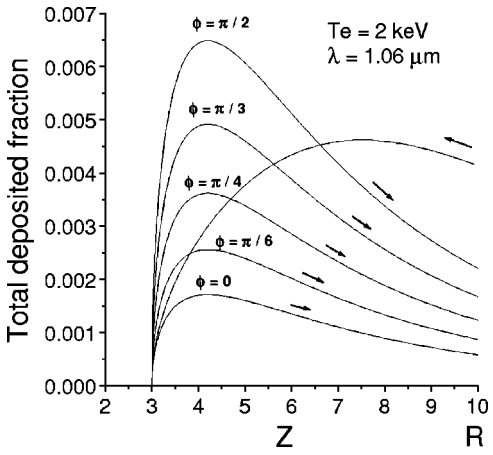

FIG. 3. Deposited fraction including IB and resonance absorption vs propagating depth of ray with wavelength 1.06 μm for 2 keV electron temperature.

that the absorption fraction in the corona increases, the reflected energy of rays decreases, and the resonance absorption disappears for 2 keV temperature and 0.53 μm wavelength [Fig. 4(a)]. On shortening the wavelength further to 0.35 μm, the energy of the rays is depleted before they arrive at the turning point and the absorption fraction in the corona

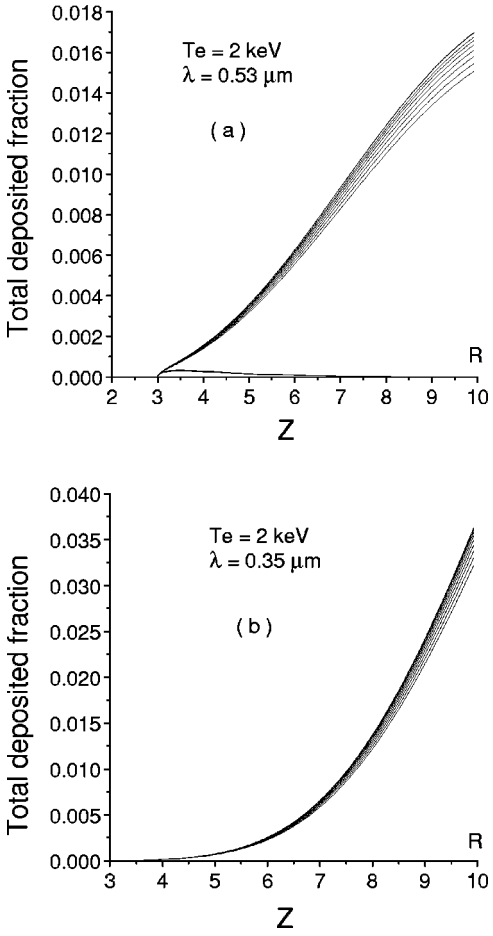

FIG. 4. Same as Fig. 2(b) but light wavelengths are (a) 0.53 μm and (b) 0.35 μm.

increases further [Fig. 4(b)]. This implies that the absorption efficiency and uniformity can be improved and the resonance absorption that leads to deposition nonuniformity can be avoided by using shorter wavelength light (e.g., $\lambda = 0.53$ or $0.35\ \mu$m). This is particularly important for laser-driven fusion.

IV. CONCLUSION

In conclusion, we suggest a more convenient and efficient 3D ray-tracing method that can greatly simplify the tracing procedures and shorten the computational time. By applying this tracing method to compute the energy deposition of a laser in a spherically symmetric plasma, we show that, increasing the fraction of IB absorption and avoiding resonance excitation during beam propagation so as to reach a high efficiency and uniformity of deposition finally, in addition to using a short wavelength of the laser, low temperature of the plasma is also a significant dynamical factor.

ACKNOWLEDGMENTS

This work was supported by the National Natural Science Foundation of China under Grant Nos. 10074009 and 19735002, and by the Foundations of the National Hi-Tech ICF Committee and the Chinese Academy of Engineering Physics.

[1] J. Lindl, Phys. Plasmas **2**, 3933 (1995).
[2] S. Skupsky and K. Lee, J. Appl. Phys. **54**, 3662 (1983).
[3] Y. V. Afanas'ev, E. G. Gamalii, N. N. Demchenko, O. N. Krokhin, and V. B. Rozanov, Zh. Éksp. Teor. Fiz. **79**, 837 (1980) [Sov. Phys. JETP **52**, 425 (1980)].
[4] L. D. Landau and E. M. Lifshitz, *Electrodynamics of Continuous Media* (Addison-Wesley, Reading, MA, 1966).
[5] E. Mazzucato, Phys. Fluids B **1**, 1855 (1989).
[6] T. B. Kaiser, Phys. Rev. E **61**, 895 (2000).
[7] M. Born and E. Wolf, *Principles of Optics* (Pergamon, Oxford, 1964).
[8] M. Kline and I. W. Kay, *Electromagnetic Theory and Geometrical Optics* (Interscience, New York, 1965).
[9] J. R. Rice, *Numerical Methods, Software, and Analysis* (McGraw-Hill, New York, 1983).
[10] T. W. Johnston and J. M. Dawson, Phys. Fluids **16**, 722 (1973).
[11] W. L. Kruer, *The Physics of Laser Plasma Interaction* (Addison-Wesley, Redwood City, CA, 1988).